Distribution Agreement

In presenting this thesis as a partial fulfillment of the requirements for a degree from Emory University, I hereby grant to Emory University and its agents the non-exclusive license to archive, make accessible, and display my thesis in whole or in part in all forms of media, now or hereafter now, including display on the World Wide Web. I understand that I may select some access restrictions as part of the online submission of this thesis. I retain all ownership rights to the copyright of the thesis. I also retain the right to use in future works (such as articles or books) all or part of this thesis.

Ronake A. Desai March 23, 2021

Characterization of growth in a galactose-1-phosphate uridylyltransferase-null rat model of classic galactosemia

By

Ronake A. Desai

Dr. Judith L. Fridovich-Keil

Adviser

Center for the Study of Human Health

Dr. Judith L. Fridovich-Keil

Adviser

Dr. Amanda A. H. Freeman

Committee Member

Dr. José D. Soria

Committee Member

2021

Characterization of growth in a galactose-1-phosphate uridylyltransferase-null rat model of classic galactosemia

By

Ronake A. Desai

Dr. Judith L. Fridovich-Keil

Adviser

An abstract of
a thesis submitted to the Faculty of Emory College of Arts and Sciences
of Emory University in partial fulfillment
of the requirements of the degree of
Bachelor of Arts with Honors

Center for the Study of Human Health

2021

Abstract

Characterization of growth in a galactose-1-phosphate uridylyltransferase-null rat model of classic galactosemia

By Ronake A. Desai

A common long-term complication in treated children and adolescents with classic galactosemia (CG) is growth delay. Growth has been evaluated in multiple studies of human patients, and decreased height and weight is delayed in children and adolescents but normalized by adulthood. In the present study, we utilized our GALT-null rat model to test for growth differences between WT and GALT-null rats at multiple pre-pubertal time points. We assessed total body mass at discrete times and percent change in mass over multiple intervals of time. Using these metrics, we have characterized growth in our model and observed that total body mass in GALT-null rats is decreased compared to WT rats at discrete time points and that GALT-null rats experience a delayed pre-pubertal growth spurt.

Characterization of growth in a galactose-1-phosphate uridylyltransferase-null rat model of classic galactosemia

By

Ronake A. Desai

Dr. Judith L. Fridovich-Keil

Adviser

A thesis submitted to the Faculty of Emory College of Arts and Sciences
of Emory University in partial fulfillment
of the requirements of the degree of
Bachelor of Arts with Honors

Center for the Study of Human Health

2021

Acknowledgements

I am extremely grateful to all members of the Fridovich-Keil Lab for their support and encouragement throughout this project. Since joining the lab in September 2018, I have felt so much warmth and camaraderie within our group, and I am so thankful for the opportunity to work with so many inspiring peers. I am especially grateful to Dr. Fridovich-Keil for allowing me to take part in her research and complete this thesis. Without her unlimited support and guidance, this project would not have been possible. Many thanks are given to Dr. Shauna A. Rasmussen and other current and former members of our group who made this project possible by assisting with the weighing of rats from 2017 to 2019. Notably, Sneh Patel assisted with statistical analyses and the construction of data figures, and I am so thankful for his diligence and patience throughout this project. Additional thanks to Taylor Head, MS, for her prior weight analyses that initiated our understanding of a growth phenotype in GALT-null rats. I am also thankful for Drs. Amanda Freeman and José Soria for serving on my Honors committee. Your guidance, words of wisdom, and support throughout my undergraduate studies has been paramount to my success as a student and individual. Thank you so much. Last but not least, I thank the Center for the Study of Human Health for the opportunity to pursue Honors. I have learned so much from the Human Health program, and I credit the incredible faculty in this department for nurturing my appreciation for scientific discovery.

Table of Contents

List of Figures and Tables

Chapter 1: Galactose and Classic Galactosemia

Galactose and Its Metabolism

Galactose is an aldohexose monosaccharide sugar that, in nature, exists most commonly in the D-conformation and is ubiquitous among animals, bacteria, and plants (Bell, 1962). Galactose is available both in free and bound forms. In its bound forms, galactose comprises complex carbohydrates (e.g., oligosaccharides and polysaccharides), glycoproteins, and glycolipids (Abi-Hanna & Saavedra, 1998). Importantly, galactose and glucose combine by a β-1-4 glycosidic linkage to produce lactose, a disaccharide sugar prevalent in animal milks that serves as a critical energy source for newborns (Berg et al., 2002; Coelho et al., 2015). Thereby, for humans, lactose in maternal milk consumed during nursing and through consumption of dairy products (e.g., yoghurts, milks, cheeses, etc.) provides a significant dietary source of galactose.

In humans and other mammals, lactose is hydrolyzed by enterocytes via the disaccharidase lactase-phlorizin hydrolase into its constituent monosaccharides, galactose and glucose (Abi-Hanna & Saavedra, 1998). Both of these monosaccharides are actively transported across the intestinal brush border membrane through the Na^+-glucose transporter or the symporter sodium/glucose co-transporter 1 (SGLT1). Two Na^+ ions bind the outer surface of the transporter, producing a conformational change that enables galactose (or glucose) to bind the inner surface. Galactose is then released by the transporter into the enterocytic cytoplasm, effluxes from the enterocyte, and enters the portal vein where it is transported to the liver. In the liver, glucose transporter 2 (GLUT2) has a high capacity to bind galactose; additionally, galactokinase (GALK) phosphorylates galactose to galactose-1-phosphate (Gal-1-P). On average, 88% of galactose remains in the liver and the rest is disseminated to other tissues.

In aqueous solution, galactose assumes either of two predominant anomeric forms: α- or β-pyranose (Coelho et al., 2015). Upon hydrolyzation from lactose, galactose assumes the β-conformation and is converted into the α-pyranose conformation by galactose mutarotase (GALM). This conversion is key because it enables galactose to enter the Leloir pathway, the predominant pathway for galactose metabolism. The Leloir pathway metabolizes galactose through the action of three enzymatic reactions (Holden et al., 2003). In the first reaction, galactose is phosphorylated via GALK to form Gal-1-P. In the second reaction, galactose-1-phosphate uridylyltransferase (GALT) catalyzes two molecular reactions: 1) the liberation of glucose-1-phosphate (Glc-1-P) from uridine diphosphate-glucose (UDP-glc), and 2) the addition of galactose-1-phosphate (Gal-1-P) to the residual uridine monophosphate (UMP) to generate uridine diphosphate-galactose (UDP-gal). In the final reaction, UDP-galactose 4'-epimerase (GALE) catalyzes the interconversion of UPD-glc and UPD-gal.

Alternatively, three non-Leloir enzymatic pathways may also conduct galactose metabolism (Walter & Fridovich-Keil, 2008). These accessory pathways include: 1) the conversion of galactose to galactitol via aldose reductase, 2) the conversion of galactose to galactonate by galactose dehydrogenase, and 3) the conversion of Gal-1-P to UDP-gal by UDP-glucose/galactose pyrophosphorylase (UGP). UDP-gal and UDP-glc serve as "sugar donors" of glycosylation reactions and are critical for the production of glycoconjugates. Glc-1-P produced from the conversion of Gal-1-P via GALT leads to the production of Glc-6-P and glucose, essential carbohydrates for energy.

Classic Galactosemia (CG)

Classic galactosemia (CG) is a rare, autosomal recessive genetic condition affecting 1 in 50,000 live births in the United States (Berry, 2020). CG is observed worldwide and its prevalence varies across populations. CG results from homozygous loss of function mutations in the *GALT* gene, producing profound deficiency of galactose-1-phosphate uridylyltransferase (GALT), the second enzyme of the Leloir pathway. GALT deficiency disrupts the metabolism of galactose, leading to the toxic accumulation of galactose, galactitol, and Gal-1-P within cells, tissues, and organ systems. It is hypothesized that the abnormal accumulation of these metabolites underlies acute and long-term outcomes in CG. Although, it remains unknown which metabolite or metabolites are causally implicated in tissue-specific insult.

If human infants with CG are not immediately and diligently treated with a low-galactose diet, life-threatening consequences arise only days after nursing onset (Pyhtila et al., 2015). The clinical presentation of CG begins within the first few days of life among infants who are breastfed or receive infant formula containing lactose. Following galactose exposure from milk or formula, the vast majority of infants with CG experience rapidly-worsening symptoms over days to weeks, including vomiting, failure to thrive, hepatocellular damage, sepsis from *Escherichia coli*, and acute neonatal mortality (Walter & Fridovich-Keil, 2008). This acute galactose toxicity can be prevented or reversed by rapid dietary restriction of galactose, typically accomplished by immediately switching an infant from breastmilk or lactose-containing formula to a non-dairy formula with only minimal galactose (e.g., soy-based formula) (Pyhtila et al., 2015).

With the advent of newborn screening (NBS) for CG, early diagnosis and intervention can be achieved, preventing affected infants from developing acute CG symptoms (Pyhtila et al., 2015). However, despite early identification and intervention through a galactose-restricted diet,

more than half of all CG patients develop a multitude of long-term complications. These long-term outcomes include cognitive impairment, speech delay, motor impairment, primary ovarian insufficiency with accompanying infertility, and growth delay (Frederick et al., 2017; Pyhtila et al., 2015).

Normal Early Growth in Humans

The Centers for Disease Control and Prevention (CDC) has characterized normal growth in children and young adults in the United States, and growth charts for boys and girls with weight-for-age and stature-for-age have been produced (*Growth Charts – Data Table of Stature-for-Age Charts, 2019)* (see Supplementary Figures 1 and 2). A marked period of growth occurs during puberty; this pubertal growth spurt is a rapid and intense increase in the rate of growth in both height and weight that occurs during the adolescent stage of the human life cycle (Bogin, 1999). This growth spurt (height), a notable feature of human puberty, but not its only defining characteristic, begins on average at 10 years in girls and 12 years in boys. The intensity and duration of the growth spurt is typically greater among boys, accounting for the sexual dimorphism in height and weight observed between adult men and women.

Using data from the CDC (*Growth Charts - Data Table of Stature-for-Age Charts*, 2019), we evaluated 50th percentile weight-for-age and height-for-age through yearly percent change in total mass and height for males and females ages 2-18 years (Supplemental Figures 4-7). We observed that males experience a peak percent change in mass at age 11 years (11.31%) and a peak percent change in height at age 13 years (4.71%). Among females, these peaks occurred at age 9 years for mass (11.86%) and age 11 years for height (4.77%). Through these findings, we can extrapolate that there are discrete changes occurring in the acquisition of mass and height that may likely begin prior to other aspects of puberty.

Growth Delay in Patients with CG

An important and relevant long-term complication of CG is growth delay or growth retardation. The mechanisms of growth delay in CG have not been elucidated, however hypotheses postulate that patients may be at risk for abnormal growth due to intrinsic disease-related factors (e.g., delayed puberty), factors related to dietary restriction and galactose/lactose avoidance, reduced caloric extraction efficiency from food, and a perturbed gut microbiome that hampers digestion. It is generally agreed that growth delay in CG has multiple etiologies. Growth delay in CG has been described in multiple studies of human patients (Frederick et al., 2017; Panis et al., 2007; Waggoner et al., 1990).

Studies of postnatal growth in CG are clear: growth is delayed among affected children and adolescents, but the story is complicated. In a study of 40 affected patients, mean height adjusted for target height was decreased among males and females, and females were more affected (Panis et al., 2007). Additionally, height growth velocities were correlated with decreased insulin-like growth factor 1 (IGF-I) Z-score, insulin-like growth factor binding protein 3 (IGFBP-3) Z-score, and height Z-score corrected for target height Z-score, and predicted final weights were less than target weights in the majority of patients. Height and weight growth velocities as well as mean height corrected for target height were decreased among both males and females, and females were more affected for both (Panis et al., 2007). In 5 patients who continued to grow after 18 years of age, target height was achieved. In another study, growth in 350 affected patients was shown to be delayed for both height-for-age and weight-for-height measurements (Waggoner et al., 1990). Growth height-for-age percentiles were severely delayed during childhood and early adolescence (from birth to 16 years of age) but were normalized throughout the late teens such that final adult heights were normal (Waggoner et al., 1990). Mean height-for-age percentiles were significantly lower among females than males from ages 5-12

years and one third (31/93) of females were below the 3rd percentile in height-for-age compared to 9 of 72 (12%) of males, illustrating more severe delay in female patients in this age group. Mean weights-for-height at <1 year, 1 year, 2-4 years, and 5-9 years ranged from the 34th to 43rd percentiles among both males and females (Waggoner et al., 1990).

Additionally, a study conducted by Frederick and colleagues (2017) evaluated the severity of long-term outcomes in CG as a function of how completely galactose was restricted from patients' diets. Affected patients 12-16 years old, regardless of the rigor of dietary restriction of galactose, displayed statistically significant decreased height Z-score differentials from mid-parental height predictions as compared to unaffected controls. Additionally, Frederick and colleagues found that rigor of dietary galactose restriction did not associate with the severity of *any* measured long-term outcomes, including height, use of speech therapy, use of special education services, adaptive function, and Anti-Mullerian hormone (AMH) among females. Importantly, these findings demonstrate that a therapeutic approach to CG that relies solely on dietary restriction of galactose, regardless of the rigor of restriction, is not associated with a reduction in the severity of long-term outcomes in CG, including growth delay.

To date, there are contradictory and incomplete findings regarding prenatal growth among CG patients. In one study of 45 affected patients, mean birth weight was 0.30kg (10.5 oz) lower than unaffected siblings, and among infants who failed to thrive, mean birth weight was 0.42kg (14.8 oz) lower than unaffected siblings (Hysia & Walker, 1961). These findings have not been observed in other studies of growth in CG patients and their unaffected siblings, and mean length and weight at birth have shown to fall within unaffected population reference ranges. Thus, it remains unclear and unknown whether events during gestation may produce growth restriction in pregnancies involving fetuses with CG (Panis et al., 2007; Waggoner et al., 1990).

CG patients also exhibit delayed puberty. In females, hypergonadotropic hypogonadism leads to delayed puberty, primary amenorrhea (failure to initiate menstruation by age 14), and primary ovarian insufficiency (Frederick et al., 2018; Gubbels et al., 2008). In males, levels of testosterone, luteinizing hormone (LH), and follicle stimulating hormone (FSH) suggest pubertal delay, but have not been extensively studied and are unknown to be associated with reproductive pathology in CG (Schweitzer et al., 1993; Waggoner et al., 1990). Though a likely possibility, it has not yet been elucidated whether delayed puberty is an etiological factor for growth delay in CG, and this remains an open question.

Chapter 2: Mammalian Models of GALT-Deficiency

The History of GALT Deficient Rodent Models

Animal models, particularly mammalian models, are often used to facilitate studies of mechanism and to test candidate interventions in genetic disease (Vandamme, 2014). In this chapter, we will review GALT-null models for CG generated in inbred strains of mice and in one outbred strain of rat.

The first GALT-deficient mouse model was developed in 1996 through gene targeting to study pathogenesis and pathophysiology in CG, but it failed to replicate common human phenotypes (Leslie et al., 1996). Biologically, this model displayed biochemical markers of CG including elevated Gal-1-P in the liver and red blood cells and elevated levels of galactose in plasma. Female GALT-null mice displayed normal reproductive function, achieved pregnancy quickly upon mating, and produced viable pups of normal size and number, suggesting that this model did not replicate ovarian insufficiency or reproductive disruption as observed in female CG patients. Though this model showed some biochemical markers of CG (elevated Gal-1-P and galactose), it did not model other patient phenotypes, including growth delay and ovarian insufficiency (Leslie et al., 1996).

A different GALT-null mouse was developed in 2014 using *GALT* gene-trapped embryonic stem cells injected into blastocysts and inserted into female mice (Tang et al., 2014). This model of CG was developed to test a novel therapy intended to reduce the accumulation of Gal-1-P, a toxic metabolite of galactose hypothesized to contribute to long-term CG outcomes. In contrast to the model developed by Leslie et al. (1996), this stem-cell-based model by Tang et al. (2014) reportedly presented features typical of CG including abnormally elevated levels of galactose and Gal-1-P in red blood cells and an impaired reproductive phenotype indicated by

smaller litter size, longer time until pregnancy, and reduced quantities of ovarian follicles. In galactose intoxication studies in this model, mothers of GALT-deficient pups were fed a high-galactose (40%) diet after their pups were born to ostensibly elevate quantities of galactose in maternal milk (Tang et al., 2014). This maternal high-galactose diet resulted in mortality in 70% of GALT-deficient pups. This effect was not observed in wild-type (WT) or heterozygous pups. Pups who survived galactose intoxication ostensibly from maternal milk displayed severe growth restriction, even when fed normal chow after weaning, and pups whose nursing mothers were not exposed to extra galactose also demonstrated growth restriction.

Of concern, growth rate and weight of both WT and GALT-deficient mice was decreased following exposure to 20% galactose diet after birth (Tang et al., 2014). This finding suggests that growth restriction in CG might not fully be explained by the inability of individuals with CG to extract calories and nutrients from galactose in food and milk and rather toxicity of galactose and its metabolites may also contribute. The relevance of growth phenotypes on this diet to human disease outcomes must also be questioned because patients with CG experience growth delay on galactose-restricted diets that do not associate with delay in their genetically normal or heterozygous peers.

Most recently, a GALT-null Sprague-Dawley rat model of CG was developed using CRISPR-Cas9 gene editing with non-homologous end joining to introduce a 2-base pair mutation in exon 6 of the *Galt* (the rat gene) locus (Rasmussen et al., 2020). This model, SD-$GALT^{M3}$, was developed in collaboration by the Fridovich-Keil Laboratory at Emory University and the Geurts Laboratory at the Medical College of Wisconsin, and is the same model used in the present study of growth in GALT-null rats. This model displays relevant phenotypic and biochemical outcomes observed in human patients with CG, including ocular cataracts, cognitive impairment,

motility impairment, and restricted growth. The WT Sprague-Dawley rat displays strong GALT activity and only baseline levels of galactose, galactitol, and Gal-1-P in relevant tissues. The SD-*GALT*^{M3} rat displays no detectable GALT activity and abnormal, increased levels of galactose, galactitol, and Gal-1-P in relevant tissues and/or plasma. Of note, both rats and humans accumulate abnormal levels of galactitol when GALT is deficient, but mice do not, owing to much lower levels of aldose reductase in mice compared with humans and rats (Rasmussen et al., 2019). Interestingly, GALT-null rats showed that the relative proportions of galactose and its metabolites differ across tissues and these proportions change over time. This finding is important because it suggests that galactose metabolites accumulate to different levels based upon tissue type, and this accumulation also changes across the course of life. This may offer a glimpse into how certain organ systems may be more resilient or vulnerable to toxic damage from galactose and its metabolites, offering valuable insight for novel therapies. Another important conclusion of studies in this rat model is that increased levels of Gal-1-P in red blood cells, a common biochemical marker measured in human patients, does not reflect localized tissue-level metabolic abnormalities. This finding raises the concern that conventional red blood cell Gal-1-P testing for human patients with CG may not be reflective of tissue-level Gal-1-P accumulation. Because this CRISPR-Cas9-based model of GALT deficiency reflects relevant patient outcomes, it is a suitable model for the exploration of mechanism, pathophysiology, and candidates for intervention and treatment in CG.

Previous Growth Findings in the SD-GALT^{M3} Model of GALT Deficiency

Our SD-*GALT*^{M3} model has previously shown growth delay among both males and females compared to WT and heterozygous rats (Rasmussen et al., 2020). Specifically, 1-day old male and female GALT-null rats showed significantly lower total body mass compared to both WT and heterozygous rats, and this trend was also observed at age 21-days old (Rasmussen et

al., 2019). At 6 weeks of age, male GALT-null rats still showed lower total body mass than wild type and heterozygous male rats but the difference was diminished and female GALT-null rats were on par with wild type and heterozygous female rats. These findings approximate the progression of growth delay in humans with CG because they show that growth, as measured by total body mass, is decreased among GALT-null rats at discrete time points during the early postnatal period, but with time, these differences diminish or are erased entirely. We also observed, as has been reported previously (Chahoud & Paumgartten, 2009), that masses of WT and GALT-null rats are highly dependent upon litter size. This ostensibly occurs because in larger litters, pups compete with one another for their mother's milk and this competition leads to each pup receiving less milk. Contrastingly, among smaller litters, competition for milk is reduced. To account for these differences, we have utilized linear mixed effects models in our analyses that adjust for differences in litter size among pups.

These previous growth findings lead to additional questions about growth in our model that the present study sought to address. Specifically, novel questions include whether growth as measured by total body mass is different between WT and GALT-null male and female rats at discrete ages, whether total body mass is altered in our model at additional discrete ages between 1-21 days, and whether percent change in total body mass over various intervals of time is different between WT and GALT-null rats. To be clear, we chose these time points simply to subdivide this period of pre-wean development into smaller segments, and not to separate known time periods of physiological development. We hypothesized that GALT-null rats would display decreased total body mass at the time points we measured and that an analysis of percentage change in mass over multiple intervals of time would demonstrate restricted and/or delayed growth. Through the present study, we have answered the above questions by testing pre-

pubertal growth in GALT-null rats to determine whether our model mimic the growth delay observed in children and adolescents with CG.

Chapter 3: Methods for Quantifying Growth Differences in GALT-null Rats

Preparation of Litters

Litters were prepared from February of 2017 to November of 2019 through crosses of WT/WT and WT/WT rats, WT/WT and GALT-null rats, GALT-null and GALT-null rats, and heterozygous and GALT-null rats. For this study, rats were defined as GALT(+) if WT or heterozygous, GALT(+/+) if WT, and GALT-null or GALT(-) if mutant.

Collection of Weight Data

All animal procedures, including maintenance and breeding, were approved by the Emory Institutional Animal Care and Use Committee (IACUC PROTO201700095; PI: JL Fridovich-Keil). All rats (Sprague-Dawley) in this study, regardless of sex or genotype, were weighed daily from ages 2- to 31-days old. Before weaning, pups were maintained with their mothers, and after weaning rats had *ad libitum* access to drinking water and chow. Pups were genotyped from tail snip DNA (at Trasnetyx) and sexed between 10-14 days old. At approximately 21-days old, pups were weaned to LabDiet 5053 and continued to be weighed daily for 10 additional days. After rats reached the age of 31-days old, they were weighed on a once-per-week basis until euthanasia. Rats were weighed using the same scale and all weights were recorded in grams. Rats with missing data, or who lost substantial weight at the assessed time points, were excluded, accounting for slight variations in sample size across analyses of the same cohort of rats.

Rat Diet

Prior to weaning, rat pups were nursed by their mothers. Rat breast milk contains approximately 3% of calories from galactose (Rasmussen et al., 2019). After weaning, rats consumed either Lab Diet 5001 or 5053 chow, which contained approximately 1% of calories from galactose.

Statistical Analysis 1: Male vs. Female Mass Comparisons of WT, Heterozygous, and GALT-null rats (Days 1-21)

The goal of this analysis was to determine whether there are significant sex-based differences in total body mass between male and female rats at ages 1-, 14-, and 21-days old. Weights at these three ages were compared within genotypes and across sex. To that end, a database with weights of all rats with data available at these time points was constructed. All weight data available at these time points were analyzed using R® (R Core Team, 2013). Individual linear mixed effects models were developed with litter size and sex as covariates (sex as the predictor variable) to quantify differences in total body mass at ages 1-, 14-, and 21-days old for male and female rats. *P*-values were deemed significant if they were less than or equal to $\alpha = 0.05$.

Statistical Analysis 2: Mass Comparisons between WT and GALT-null Rats at 1, 8, 14, and 21 Days

The goal of this analysis was to determine whether there are significant differences in total body mass at ages 1-, 8-, 14-, and 21-days old between WT and GALT-null rats using all available weight data. Data were analyzed using individual linear mixed effects models with rat genotype and litter size as covariates (genotype was the predictor variable). *P*-values were deemed significant if they were less than or equal to $\alpha = 0.05$.

Statistical Analysis 3: Weekly Percent Change in Mass (Days 1-7, 7-14, and 14-21)

The goal of this analysis was to determine whether there are significant differences in the rate of growth between WT and GALT-null rats as measured by percent change in mass over weekly intervals during the first three weeks of life using all available weight data. Data were analyzed using individual linear mixed effects models with rat genotype and litter size as covariates (genotype was the predictor variable). *P*-values were deemed significant if they were less than or equal to $\alpha = 0.05$.

Statistical Analysis 4: Daily Percent Change in Mass (Days 15-31)

The goal of this analysis was to determine whether there are significant differences in the rate of growth between WT and GALT-null rats as measured by percent change in mass on a daily basis from ages 15-days old to 31-days old using all available weight data. Data were analyzed using individual linear mixed effects models with rat genotype and litter size as covariates (genotype was the predictor variable). *P*-values were deemed significant if they were less than or equal to $\alpha = 0.05$.

Chapter 4: Results

The results presented here address three questions: 1) do male and female rats have different masses at 1, 14, and 21 days of age; 2) do GALT-null and WT rats differ in mass at 1, 8, 14, and 21 days of age; and 3) does growth, as measured by percent change in body mass differ between GALT-null and WT rats at specific time intervals during the first month of life. All figures are presented at the end of the chapter.

Male vs. Female Mass Comparisons of WT, Heterozygous, and GALT-null rats (Days 1, 14, and 21)

Among WT rats, females displayed lower total body mass at ages 1-, 14-, and 21-days old (Figure 1). At day 1, median masses for males and females were 7g and 6g respectively (IQR=1g, 2g; p=0.0029); at day 14, 30g and 29g (IQR=7g, 8.75g; p=0.0361); and at day 21, 51g and 50g (IQR=14g, 14g F; p<0.001). To be clear, we compared median mass rather than mean mass to minimize the impact of outliers, which were found in all comparison groups.

Among GALT-null rats, females displayed lower total body mass at day 1 (Figure 2). At day 1, median masses for males and females were 7g and 6g, respectively (IQR=1g, 1g F; p=0.0270); at day 14, 29g and 29g (IQR=6.75g, 7g; p=0.3542); and at day 21, 47g and 45g (IQR=12g, 12g; p=0.6299).

Mass Comparisons between Single-Sex Cohorts of WT and GALT-null Rats at 1, 8, 14, and 21 Days

Male GALT-null rats displayed lower median total body mass than their WT counterparts at ages 1-, 8-, 14-, and 21-days old (Figure 3). At day 1, median masses for WT and GALT-null rats were 7g and 6g, respectively (IQR=1g, 1g; p<0.001); at day 8, 19.0g and 17.5g (IQR=4g, 5g; p<0.001); at day 14, 31g and 28g (IQR=8g, 7g; p<0.001); and at day 21, 52g and 47g (IQR=12g, 12g; p<0.001).

Female GALT-null rats also displayed lower median total body mass than their WT counterparts at ages 1-, 8-, 14-, and 21-days old (Figure 4). At day 1, median masses for WT and GALT-null rats were 7g and 6g, respectively (IQR=1g, 1g $p<0.001$); at day 8, 18g and 17g (IQR=5g, 5g; $p=0.2938$); at day 14, 29.5g and 29g (IQR=7.5g, 7g; $p=0.03921$); and at day 21, 51g and 45g (IQR=12g, 13g; $p=0.0017$).

Weekly Percent Change in Total Body Mass (Days 1-7, 7-14, and 14-21) Among WT and GALT-null Rat Pups

Male WT rats displayed increased percent change in mass during week 3 of life (days 14-21) compared to male GALT-null rats (Figure 5). During week 1, medians for percent change in mass for WT and GALT-null rats were 128.57% and 126.79%, respectively (IQR=38.89%, 42.21%; $p=0.8533$); during week 2, 84.21% and 86.67% (IQR=17.56%, 23.07%; $p=0.7724$); and during week 3, 65.71% and 60.71% (IQR=13.74%, 16.67%; $p=0.0261$).

Female WT rats also displayed an increased percent change in mass during week 3 of life compared to female GALT-null rats (66.67% and 62.07%; IQR=16.25%, 11.55%; $p<0.001$) (Figure 6). In contrast, during week 1, medians for percent change in mass for female WT and GALT-null rats were 128.57% and 150.00%, respectively (IQR=43.65%, 54.76%; $p<0.001$); during week 2, these medians were 81.82% and 84.62% (IQR=18.75%, 19.65%; $p=0.3175$).

Daily Percent Change in Total Body Mass (Days 15-31) between WT and GALT-null Rat Pups

Male WT and GALT-null rats displayed statistically significant differences in median percent change in mass during the following intervals: 17-18 days, 19-20 days, 20-21 days, 21-22 days, and 23-24 days and exhibited peak growth on different days (WT day 20, GALT-null day 23) (Figure 7). Daily intervals before and after this key period were not significantly different between male GALT-null and WT rat pups. For 17-18 days, medians for percent change in mass for WT and GALT-null rats were 6.16% and 5.00%, respectively (IQR=4.33%,

3.45%; p=0.0181); for 19-20 days, 10.81% and 9.43% (IQR=4.15%, 5.18% p=0.0028); for 20-21 days, 11.88 and 9.68% (IQR=3.30%, 6.64%; p=0.0397); for 21-22 days, 10.82% and 10.20% (IQR=3.91%, 6.29%; p=0.0126); and for 23-24 days, 9.16% and 10.34% (IQR=3.45%, 5.05% p=0.0106).

Female WT and GALT-null rats displayed statistically significant differences in median percent change in mass during the following intervals: 19-20 days, 20-21 days, 21-22 days, and 23-24 days and exhibited peak growth on different days (WT day 20, GALT-null day 23) (Figure 8). As was observed in male rats, daily intervals before and after this period were not significantly different between female GALT-null and WT rat pups. For 19-20 days, medians for percent change in mass for WT and GALT-null female pups were 10.71% and 8.82%, respectively (IQR=3.41%, 5.11%; p=0.0150); for 20-21 days, 11.27% and 8.99% (IQR=4.44%, 4.94%; p=0.0030); for 21-22 days, 9.84% and 9.43% (IQR=4.55%, 3.60%; p=0.0252); and for 23-24 days, 8.45% and 10.42% (IQR=3.49%, 3.43% p=0.0098).

Data Figures

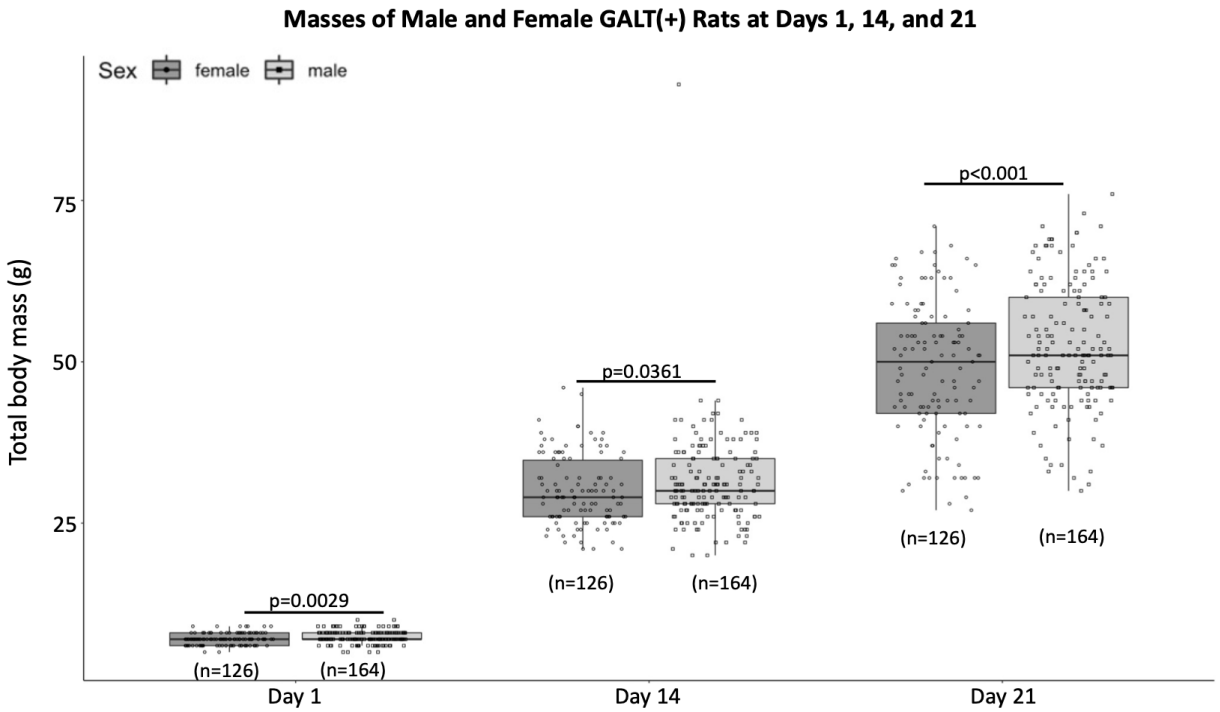

FIGURE 1: Masses of Male and Female GALT(+) Rats at Days 1, 14, and 21. Boxplots show masses of male and female GALT(+) (WT and heterozygous) rats at ages 1-, 14-, and 21-days old. P-values produced through a linear mixed effects model with sex and litter size as covariates and sex as the predictor variable and are significant at days 1, 14, and 21. Number of litters represented at Days 1, 14, and 21: 42 (males), 38 (females).

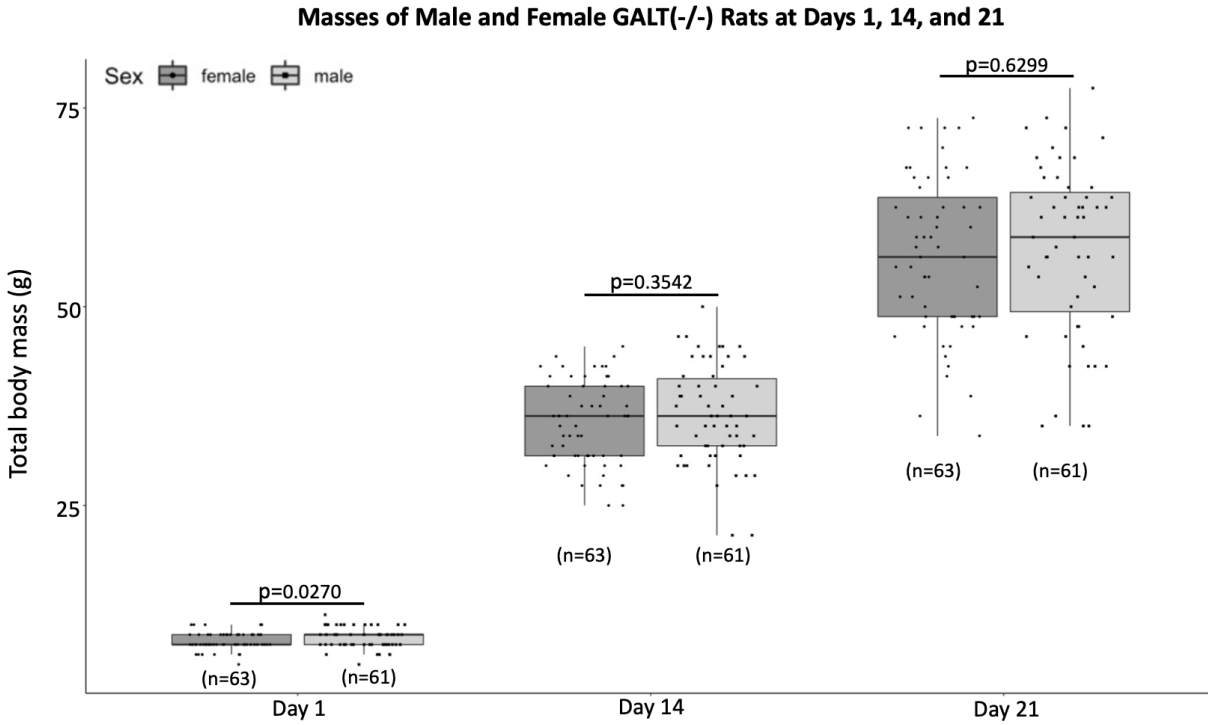

FIGURE 2: Masses of Male and Female GALT(-/-) Rats at Days 1, 14, and 21. Boxplots show masses of male and female GALT(-/-) rats at ages 1-, 14-, and 21-days old. P-values produced through a linear mixed effects model with sex and litter size as covariates and sex as the predictor variable and are significant at day 1 only. Number of litters represented at Day 1: 61 (males), 29 (females); Day 14: 32 (males), 27 (females); Day 21: 32 (males), 27 (females).

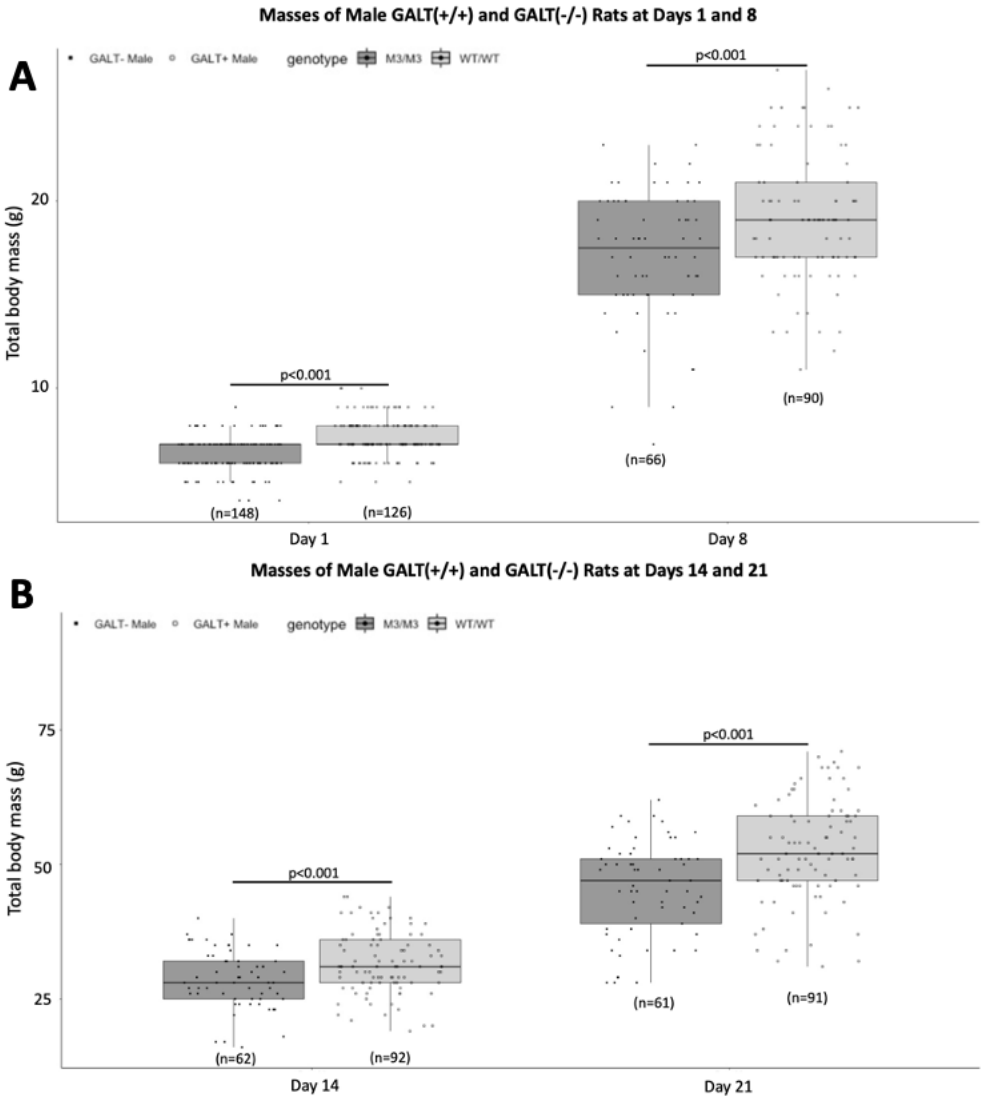

FIGURE 3: Masses of Male GALT(+/+) and GALT(-/-) Rats at Days 1 and 8 (Panel A), 14 and 21 (Panel B). Boxplots show masses at ages 1-, 8-, 14-, and 21-days old. P-values produced through a linear mixed effects model with genotype and litter size as covariates and genotype as the predictor variable and are significant at days 1, 8, 14, and 21. Number of litters represented at Day 1: 40 (GALT+/+), 66 (GALT-/-); Day 8: 32 (GALT+/+), 36 (GALT-/-); Day 14: 30 (GALT+/+), 36 (GALT-/-); Day 21: 30 (GALT+/+), 36 (GALT-/-). Cohort sizes may appear slightly different between time points due to missing data.

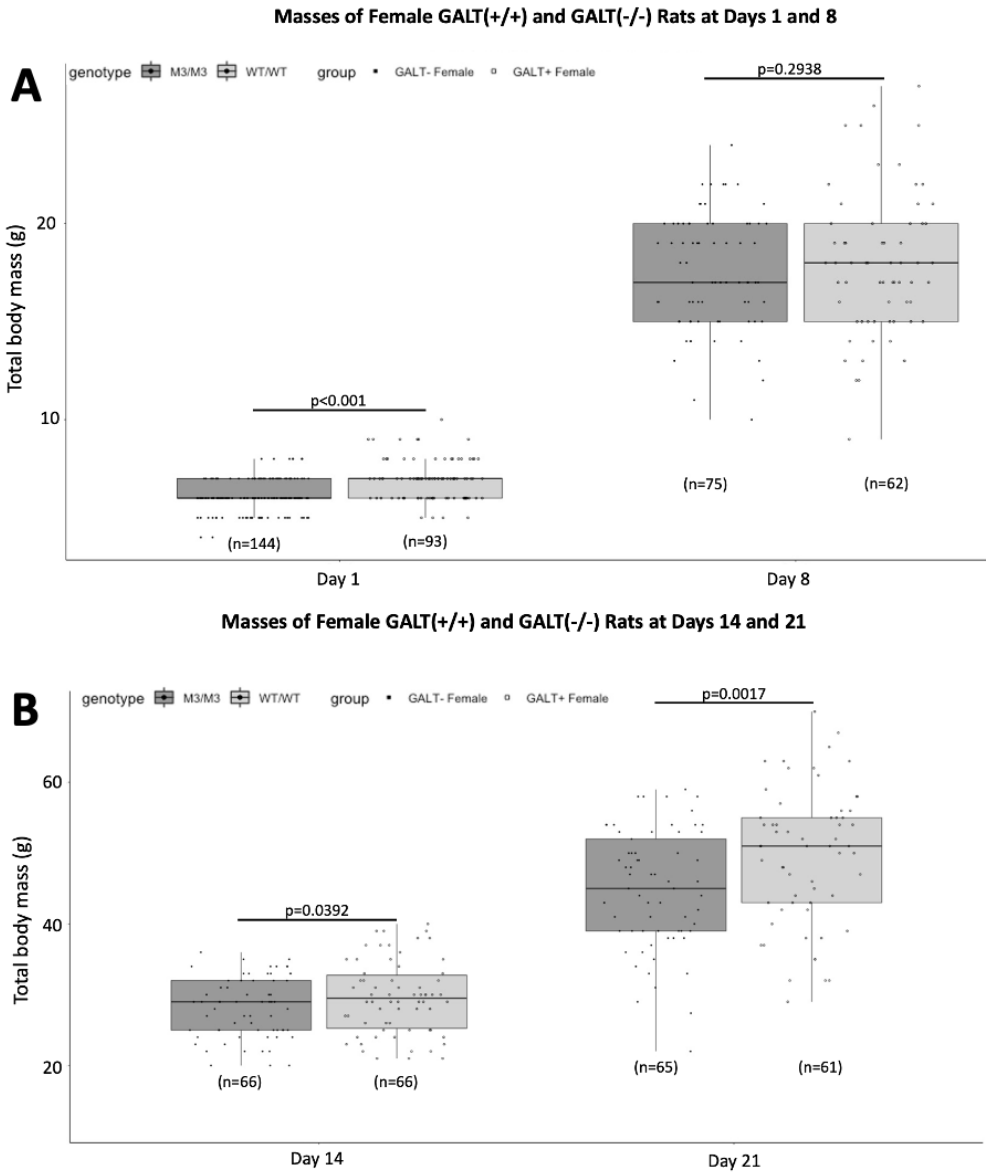

FIGURE 4: Masses of Female GALT(+/+) and GALT(-/-) Rats at Days 1 and 8 (Panel A), 14 and 21 (Panel B). Boxplots show masses at ages 1-, 8-, 14-, and 21-days old. P-values produced through a linear mixed effects model with genotype and litter size as covariates and genotype as the predictor variable and are significant at days 1, 14, and 21. Number of litters represented at Day 1: 42 (GALT(+/+)), 64 (GALT(-/-)); Day 8: 31 (GALT+/+), 36 (GALT-/-); Day 14: 30 (GALT+/+), 33 (GALT-/-); Day 21: 29 (GALT+/+), 30 (GALT-/-). Cohort sizes may appear slightly different between time points due to missing data.

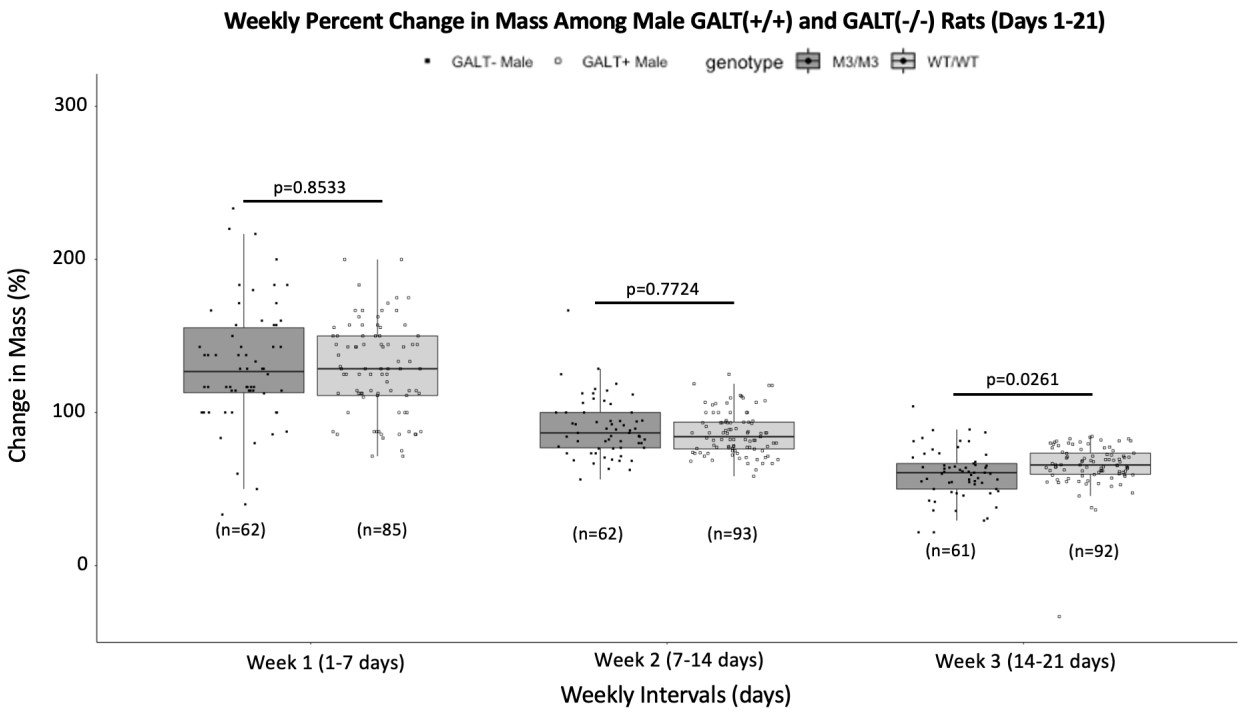

FIGURE 5: Weekly Percent Change in Mass Among Male GALT(+/+) and GALT(-/-) Rats (Days 1-21). Boxplots show percent change in mass at weeks 1, 2, and 3. P-values produced through a linear mixed effects model with genotype and litter size as covariates and genotype as the predictor variable and are significant at Week 3 only. Number of litters represented at Week 1: 28 (GALT+/+), 34 (GALT-/-); Week 2: 32 (GALT+/+), 36 (GALT-/-); Week 3: 30 (GALT+/+), 36 (GALT-/-). Cohort sizes may appear slightly different between time points due to missing data.

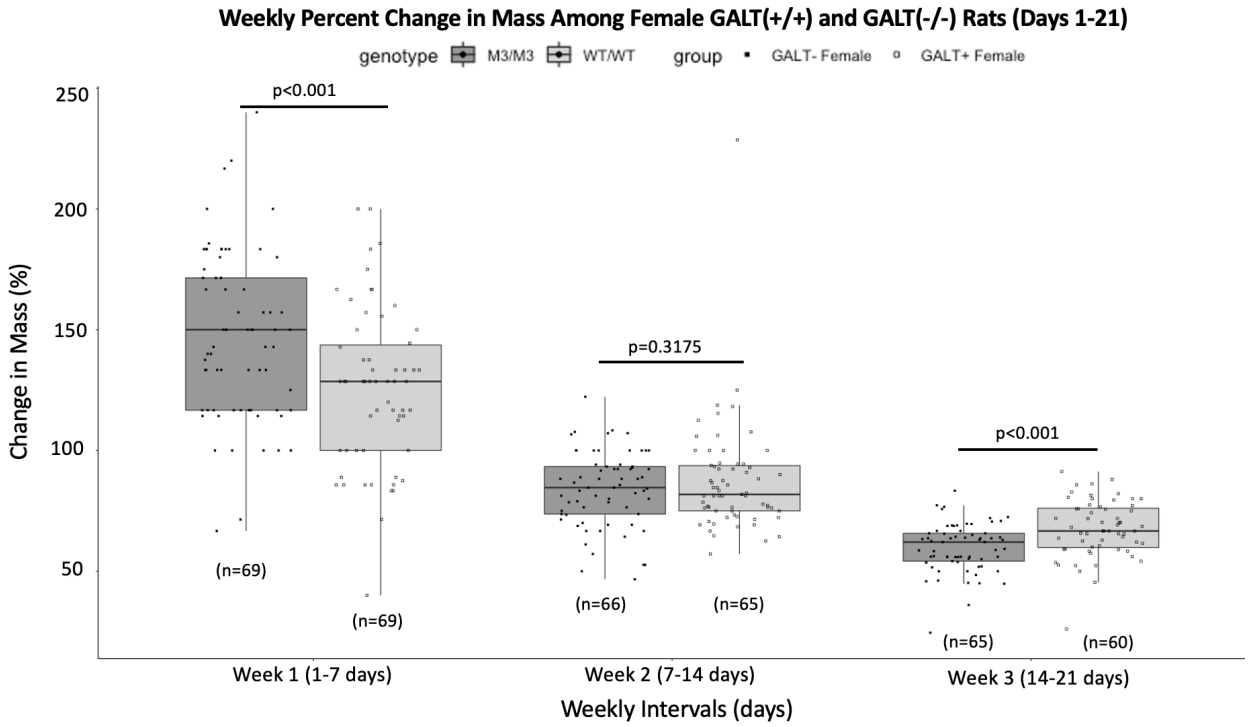

FIGURE 6: Weekly Percent Change in Mass Among Female GALT(+/+) and GALT(-/-) Rats (Days 1-21). Boxplots show percent change in mass at weeks 1, 2, and 3. P-values produced through a linear mixed effects model with genotype and litter size as covariates and genotype as the predictor variable and are significant at Week 3 only. Number of litters represented at Week 1: 31 (GALT+/+), 30 (GALT-/-); Week 2: 29 (GALT+/+), 30 (GALT-/-); Week 3: 28 (GALT+/+), 30 (GALT-/-). Cohort sizes may appear slightly different between time intervals due to missing data.

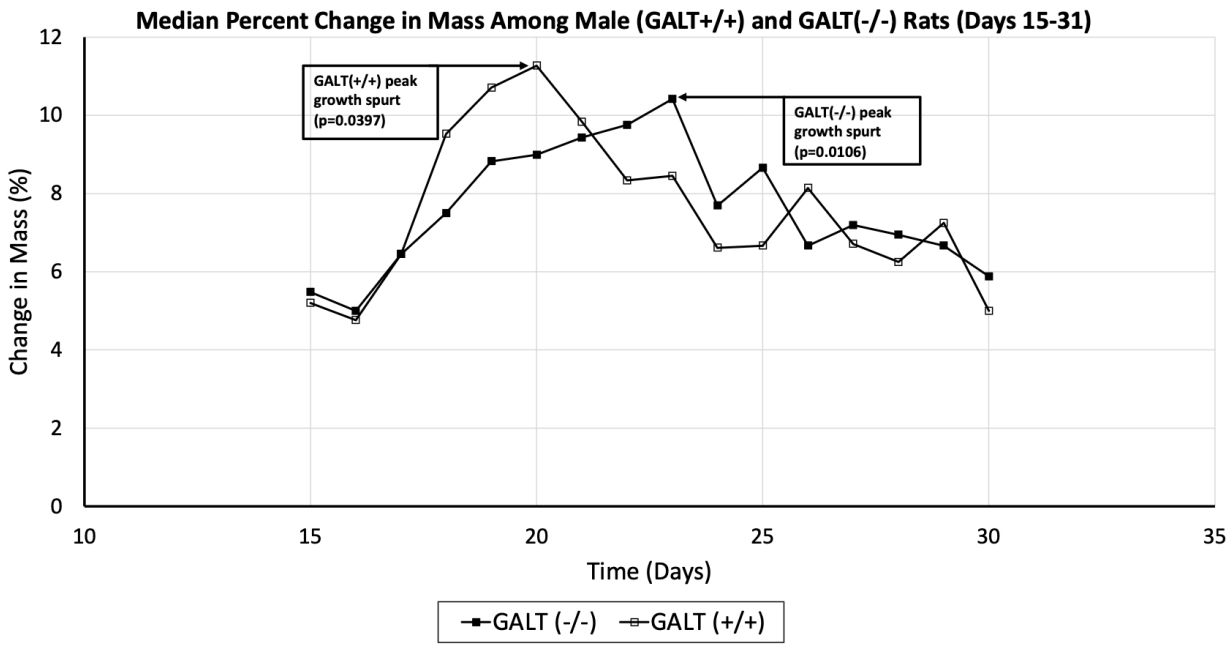

FIGURE 7: Median Percent Change in Mass Among Male GALT(+/+) and GALT(-/-) rats (Days 15-31). Lines show median percent change in mass at daily intervals from 15-31 days. P-values produced through a linear mixed effects model with genotype and litter size as covariates and genotype as the predictor variable and are significant at days 17-18, 19-20, 20-21, 21-22, and 23-24 (only shown for 20-21 and 23-24). Points of peak growth spurt indicated by arrows. Sample size (n) and number of litters represented reported in Supplementary Table 1 (Appendix).

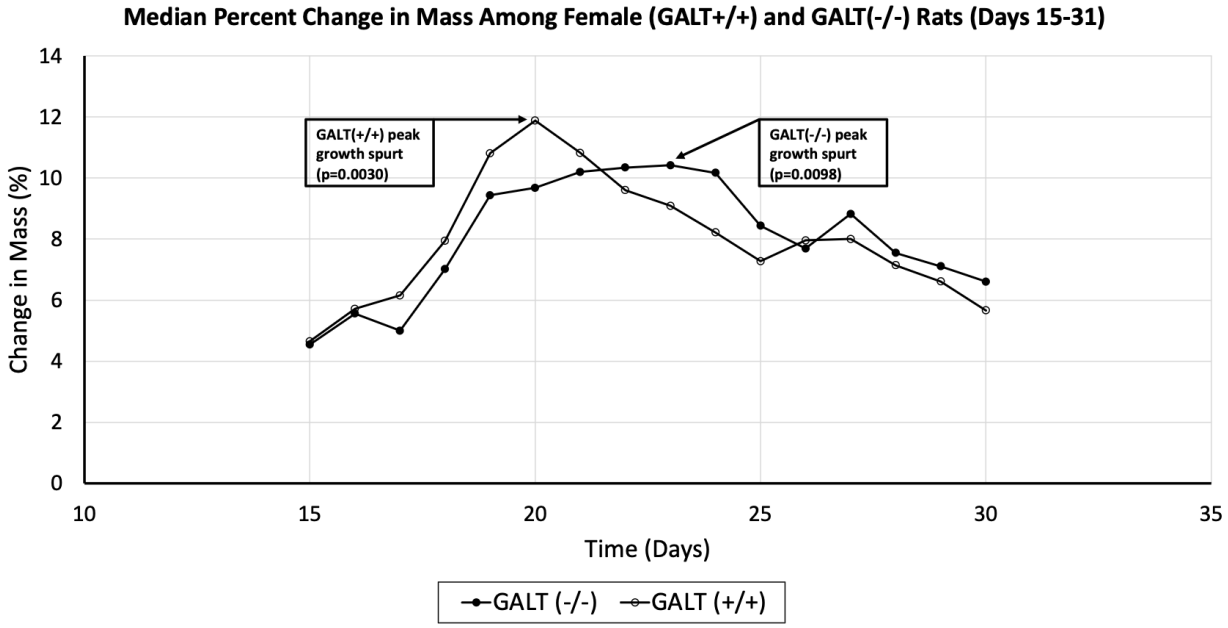

FIGURE 8: Median Percent Change in Mass Among Female GALT(+/+) and GALT(-/-) rats (Days 15-31). Lines show median percent change in mass at daily intervals from 15-31 days. P-values produced through a linear mixed effects model with genotype and litter size as covariates and genotype as the predictor variable and are significant at days 19-20, 20-21, 21-22, 23-24 (only shown for 20-21 and 23-24). Points of peak growth spurt indicated by arrows. Sample sizes (n) and number of litters represented are provided in Supplementary Table 2 (Appendix).

Chapter 5: Discussion

Here we describe a study we conducted to characterize growth within our GALT-null rat model of CG. We previously quantified growth between WT, heterozygous, and GALT-null rats at discrete time points, but gaps remained in our understanding (Rasmussen et al., 2020). In the present study, we characterized growth at additional discrete time points in our model and also applied a different approach for quantifying growth through percent change in total body mass over multiple intervals of time.

Sex is a significant predictor of mass in WT rats

At all time points measured, we observed that male and female WT rats display statistically significant differences in total mass, with males being larger. These findings serve as rationale for not combining males and females in studies of growth in our model.

Total body mass is lower in single-sex GALT-null rat cohorts at ages 1-, 8-, 14-, and 21- days

We observed that total body mass is lower in male and female GALT-null rats at all time points measured, although, among GALT-null females at day 8, results were not statistically significant. We previously observed that both male and female GALT-null rats display lower total mass at days 1 and 21(Rasmussen et al., 2020) and the present study confirms our previous findings and extends our understanding to additional early, pre-wean time points.

Weekly percent change in mass reveals a pre-pubertal growth spurt in WT and GALT-null rats

We evaluated weekly percent change in mass between GALT-null and WT rats and observed that for both males and females, critical change is occurring from 14-21 days among both males and females. We understand that there is a key dietary transition occurring during this period. Specifically, rats are starting to consume solid food in addition to maternal milk, and this dietary transition may play an important role in mass acquisition during this period. This finding prompted us to further evaluate changes during this period, and served as rationale for evaluating percent change in mass on a daily basis from 15-31 days.

Daily percent change in mass reveals time of peak pre-pubertal growth spurt is delayed in both male and female GALT-null rats

We evaluated daily percent change in mass between GALT-null and WT rats and observed that there are key points of change at specific time points. Notably, we observed that the peak point of change, characterized as the peak pre-pubertal growth spurt, occurs at day 20 for WT males and females and at day 23 for GALT-null males and females. Because our rats are typically weaned at day 21, we evaluated whether age at wean was different between WT and GALT-null rat pups and determined it was equal. Therefore, differences in time of peak pre-pubertal growth spurt cannot be explained by differences in weaning age, and is instead a real phenotype within our model. Puberty has been well-described in genetically WT Sprague-Dawley rats, but growth has not been extensively studied prior to sexual maturation (Brower et al., 2015; Campion et al., 2013; Lewis et al., 2002). In male Sprague-Dawley rats, puberty or sexual maturation generally begins between 45 and 48 days and is defined by preputial separation (separation of the prepuce from the glans penis). In females, the onset of puberty generally occurs between 32 and 34 days and is defined by vaginal opening.

We hypothesize that the differences we observe in peak pre-pubertal growth spurt between WT and GALT-null rats may potentially be a biological phenomenon of increased growth prior to puberty onset. For example, using CDC weight-for-age data in humans, we observed that 50th percentile growth shows a peak percent change in weight at age 11 years in males and at age 9 years in females. These peaks occur before the listed average age of puberty onset (age 12 years in males and age 10 years in females). This hypothesis of an early, pre-pubertal growth spurt in rats, defined by increased acquisition of mass before puberty, would follow the trend we observed in humans through analyses of CDC data on weight-for-age.

Limitations and Future Directions

In addition to many strengths, our study also had a number of important limitations. For example, all pups had *ad libitum* access to maternal milk before weaning and to rat chow after weaning at age 21-days. Rat breast milk contains 3% of calories from galactose, and solid chow contains 1.0-1.5% of calories from galactose. However, the consumed quantities of milk and chow could not be measured. This does not replicate recommendations for treated patients with CG for whom a galactose-restricted diet is the standard of care (Welling et al., 2017), and therefore, growth in rats with a truly galactose-restricted diet remains an open question. A further source of error in our study could potentially come from the involvement of multiple individuals in the weighing of rats.

Future directions include further evaluation of growth between sexes in our model. This would allow us to determine whether growth delay phenotypes presents differently between males and females in statistically meaningful ways. Additionally, we intend to study growth data in affected human patients to model their growth by weight-for-age and height-for-age at discrete time points and as a percentage change in weight or height over multiple intervals of time. Lastly, the methods described in the present study should also be applied in future studies within our model that test the utility and rescue potential of novel candidates for intervention in CG to determine whether intervention corrects the growth delay phenotypes we have described.

Appendix

Supplementary Tables and Figures

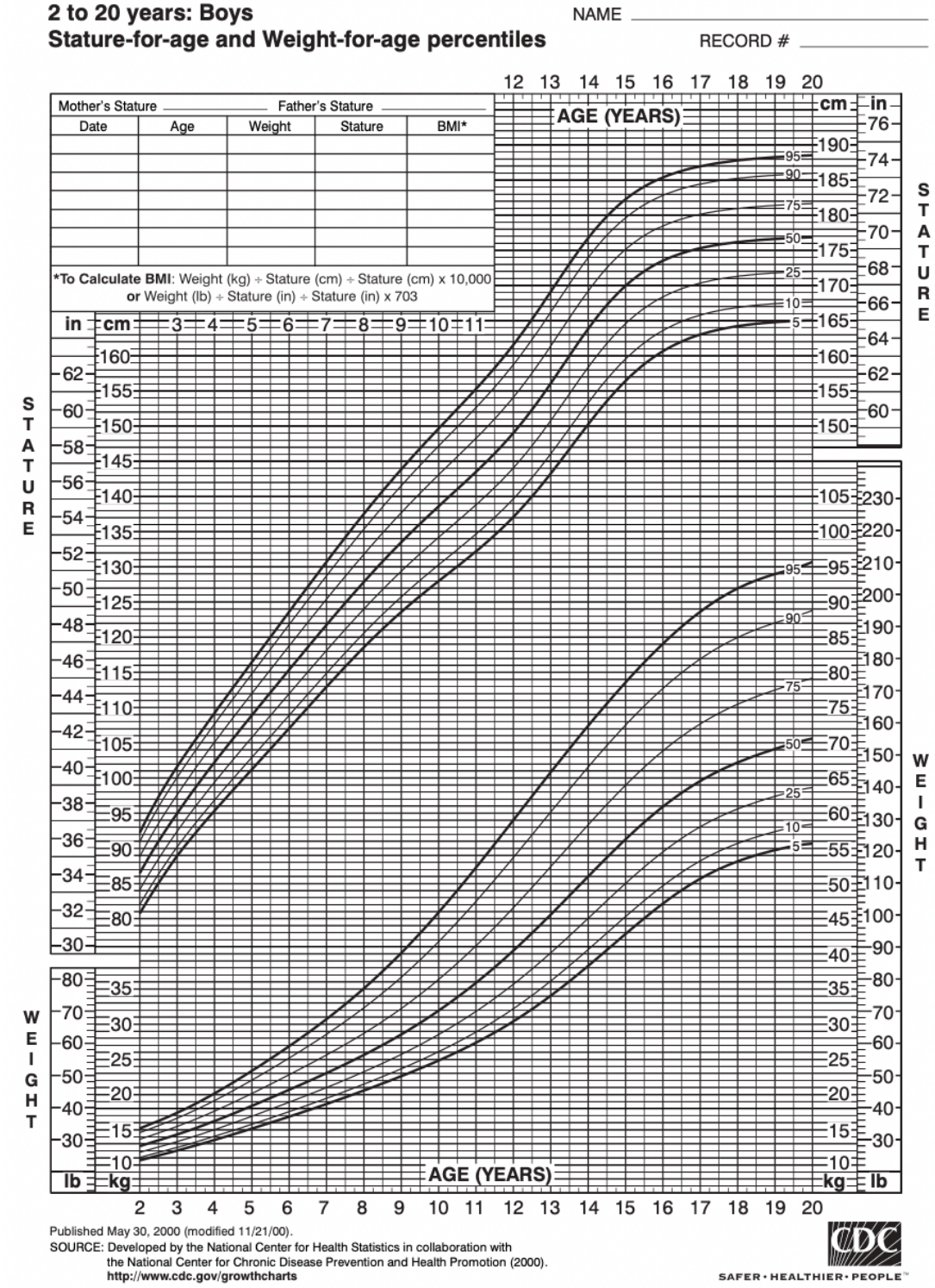

SUPPLEMENTARY FIGURE 1: CDC Growth Curves (Boys 2-20 Years). (*Growth Charts - Data Table of Stature-for-Age Charts*, 2019).

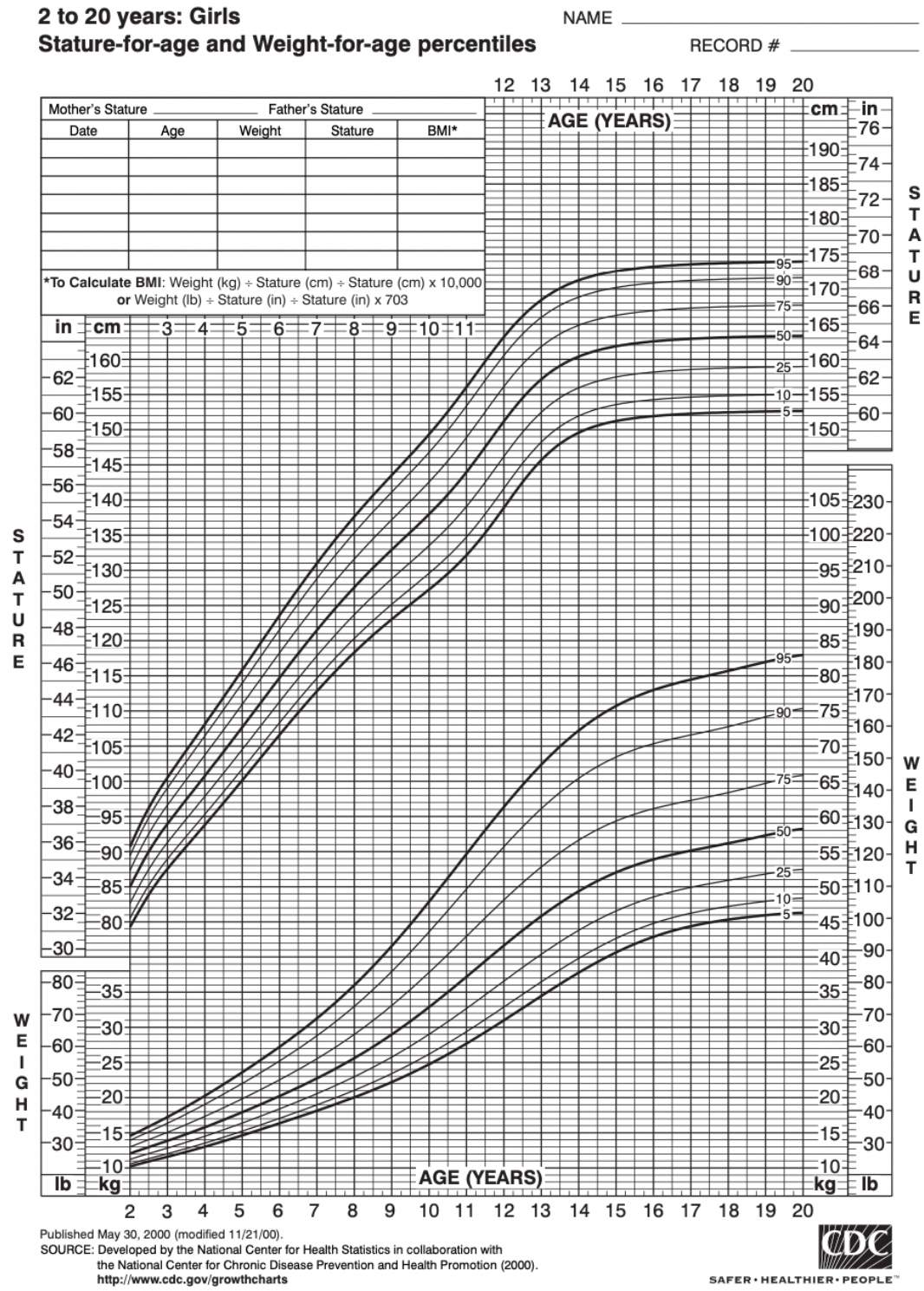

SUPPLEMENTARY FIGURE 2: CDC Growth Curves (Girls 2-20 Years). (*Growth Charts - Data Table of Stature-for-Age Charts*, 2019).

SUPPLEMENTARY FIGURE 3: Human Male Growth 2-18 Years (Year-to-Year % Change in Mass). CDC data on 50th percentile male weight-for-age was used to evaluate percent change in total body mass each year from 2-18 years (*Growth Charts - Data Table of Stature-for-Age Charts*, 2019).

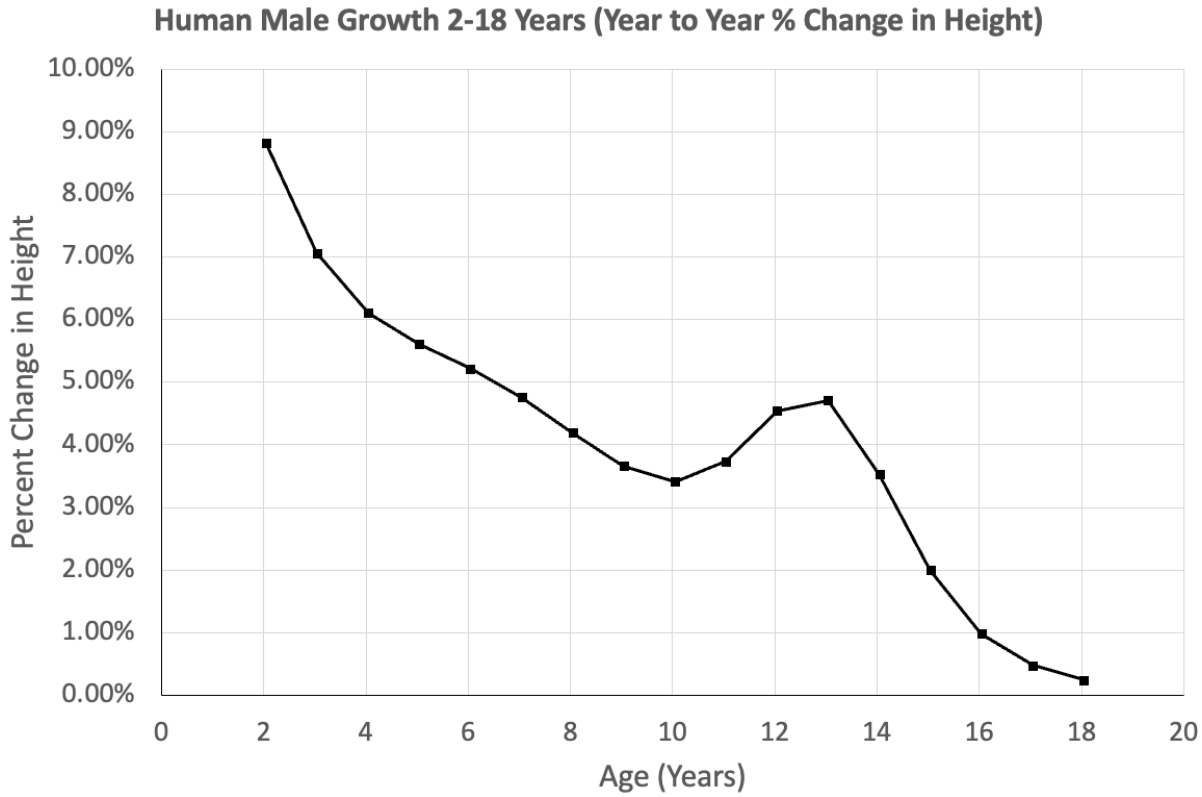

SUPPLEMENTARY FIGURE 4: Human Male Growth 2-18 Years (Year-to-Year % Change in Height). CDC data on 50th percentile male height-for-age was used to evaluate percent change in height each year from 2-18 years (*Growth Charts - Data Table of Stature-for-Age Charts*, 2019).

SUPPLEMENTARY FIGURE 5: Human Female Growth 2-18 Years (Year-to-Year % Change in Mass). CDC data on 50th percentile female weight-for-age was used to evaluate percent change in total body mass each year from 2-18 years (*Growth Charts - Data Table of Stature-for-Age Charts*, 2019).

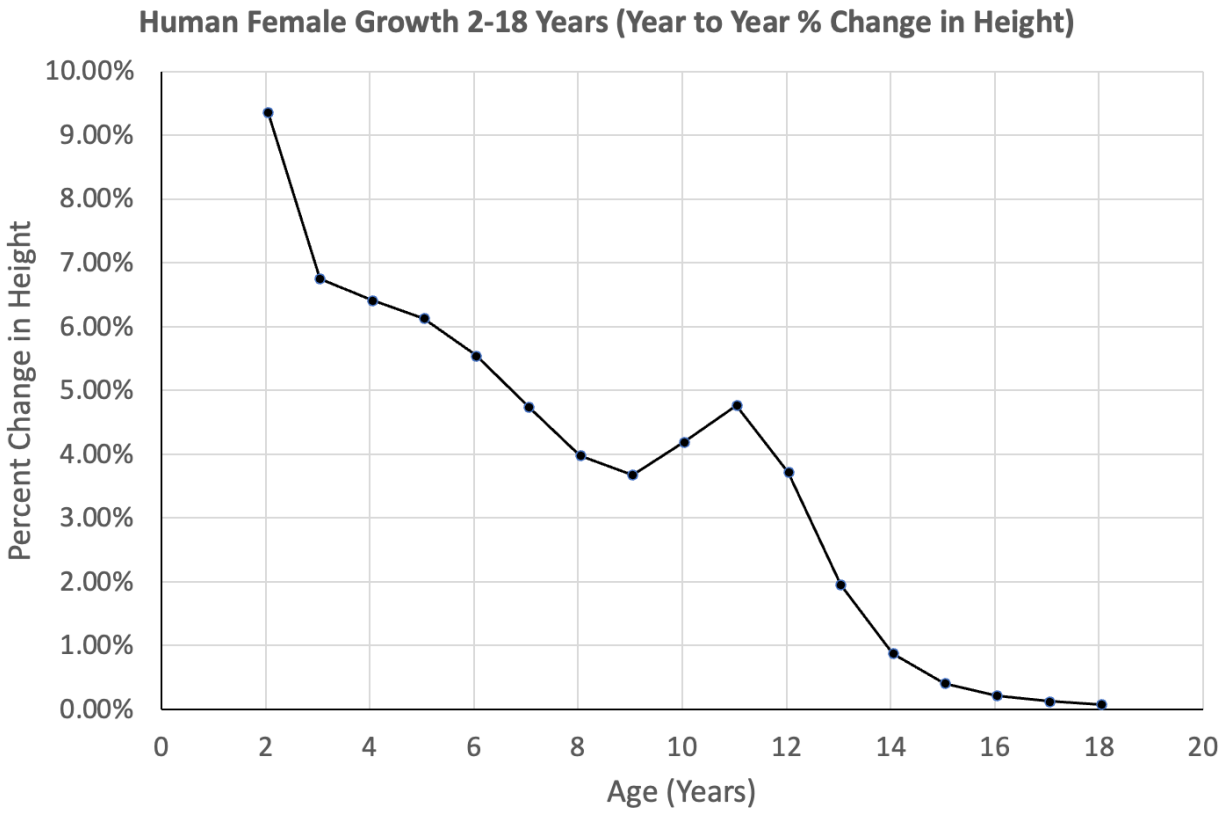

SUPPLEMENTARY FIGURE 6: Human Female Growth 2-18 Years (Year-to-Year % Change in Height). CDC data on 50th percentile female height-for-age was used to evaluate percent change in height each year from 2-18 years (*Growth Charts - Data Table of Stature-for-Age Charts*, 2019).

.

Interval	n: GALT(+/+)	# of litters (GALT(+/+)	n: GALT (-/-)	# of litters (GALT(-/-)
15-16	84	28	55	33
16-17	83	28	54	33
17-18	84	28	54	33
18-19	84	28	56	33
19-20	84	28	57	33
20-21	84	28	56	33
21-22	74	28	51	33
22-23	46	20	43	24
23-24	33	16	31	18
24-25	29	16	29	17
25-26	31	16	30	17
26-27	29	15	32	17
27-28	29	15	33	17
28-29	27	15	32	17
29-30	29	15	30	17
30-31	26	15	27	15

SUPPLEMENTARY TABLE 1: Sample Characteristics (Figure 10): Median Percent Change in Mass Among Male GALT(+/+) and GALT(-/-) rats (Days 15-31).

Interval	n: GALT(+/+)	# of litters (GALT(+/+)	n: GALT (-/-)	# of litters (GALT(-/-)
15-16	60	28	58	27
16-17	59	28	57	27
17-18	57	28	57	27
18-19	57	28	61	27
19-20	57	28	61	27
20-21	58	28	60	27
21-22	55	28	47	27
22-23	33	19	39	20
23-24	24	16	30	16
24-25	28	16	30	15
25-26	26	15	30	15
26-27	26	15	30	15
27-28	26	15	30	15
28-29	25	15	27	15
29-30	27	15	25	15
30-31	26	15	27	15

SUPPLEMENTARY TABLE 2: Sample Characteristics (Figure 11): Median Percent Change in Mass Among Female GALT(+/+) and GALT(-/-) rats (Days 15-31).

References

Abi-Hanna, A., & Saavedra, J. M. (1998). GALACTOSE*. In B. Caballero (Ed.), *Encyclopedia of Human Nutrition (Second Edition)* (pp. 377–383). Elsevier. https://doi.org/10.1016/B0-12-226694-3/00144-7

Bell, D. J. (1962). Chapter 7 - Natural Monosaccharides and Oligosaccharides: Their Structures and Occurrence. In *Comparative Biochemistry V3: A Comprehensive Treatise* (1st ed., pp. 287-354). Cambridge, MA: Academic Press. doi: 10.1016/B978-0-12-395544-9.50018-2.

Berg, J. M., Tymoczko, J. L., & Stryer, L. (2002). Complex Carbohydrates Are Formed by Linkage of Monosaccharides. *Biochemistry. 5th Edition*. https://www.ncbi.nlm.nih.gov/books/NBK22396/

Berry, GT. Classic galactosemia and clinical variant galactosemia. In: Adam MP, Ardinger HH, Pagon RA, et al., eds.*GeneReviews®*. Seattle (WA): University of Washington, Seattle; 1993. http://www.ncbi.nlm.nih.gov/books/NBK1518/. Accessed 15 March 2021.

Bogin, B. (2020). *Patterns of Human Growth* (3rd ed.). Cambridge University Press. https://doi.org/10.1017/9781108379977

Brower, M., Grace, M., Kotz, C. M., & Koya, V. (2015). Comparative analysis of growth characteristics of Sprague Dawley rats obtained from different sources. *Laboratory Animal Research*, *31*(4), 166–173. https://doi.org/10.5625/lar.2015.31.4.166

Campion, S. N., Carvallo, F. R., Chapin, R. E., Nowland, W. S., Beauchamp, D., Jamon, R., Koitz, R., Winton, T. R., Cappon, G. D., & Hurtt, M. E. (2013). Comparative assessment of the timing of sexual maturation in male Wistar Han and Sprague-Dawley rats.

Reproductive Toxicology (Elmsford, N.Y.), *38*, 16–24. https://doi.org/10.1016/j.reprotox.2013.02.003

Chahoud, I., & Paumgartten, F. J. R. (2009). Influence of litter size on the postnatal growth of rat pups: Is there a rationale for litter-size standardization in toxicity studies? *Environmental Research*, *109*(8), 1021–1027. https://doi.org/10.1016/j.envres.2009.07.015

Coelho, A. I., Berry, G. T., & Rubio-Gozalbo, M. E. (2015). Galactose metabolism and health: *Current Opinion in Clinical Nutrition and Metabolic Care*, *18*(4), 422–427. https://doi.org/10.1097/MCO.0000000000000189

Frederick, A. B., Cutler, D. J., & Fridovich-Keil, J. L. (2017). Rigor of non-dairy galactose restriction in early childhood, measured by retrospective survey, does not associate with severity of five long-term outcomes quantified in 231 children and adults with classic galactosemia. *Journal of Inherited Metabolic Disease*, *40*(6), 813–821. https://doi.org/10.1007/s10545-017-0067-x

Frederick, A. B., Zinsli, A. M., Carlock, G., Conneely, K., & Fridovich-Keil, J. L. (2018). Presentation, progression, and predictors of ovarian insufficiency in classic galactosemia. *Journal of Inherited Metabolic Disease*, *41*(5), 785–790. https://doi.org/10.1007/s10545-018-0177-0

Growth Charts—Data Table of Stature-for-age Charts. (2019, January 11). https://www.cdc.gov/growthcharts/html_charts/statage.htm

Gubbels, C. S., Land, J. A., & Rubio-Gozalbo, M. E. (2008). Fertility and impact of pregnancies on the mother and child in classic galactosemia. *Obstetrical & Gynecological Survey*, *63*(5), 334–343. https://doi.org/10.1097/OGX.0b013e31816ff6c5

Holden, H. M., Rayment, I., & Thoden, J. B. (2003). Structure and function of enzymes of the Leloir pathway for galactose metabolism. *The Journal of Biological Chemistry*, *278*(45), 43885–43888. https://doi.org/10.1074/jbc.R300025200

Hysia, D., & Walker, F. (1961). Variability in the clinical manifestations of galactosemia. *The Journal of Pediatrics*, *59*(6), 872–883. https://doi.org/10.1016/S0022-3476(61)80317-X

Leslie, N. D., Yager, K. L., McNamara, P. D., & Segal, S. (1996). A Mouse Model of Galactose-1-Phosphate Uridyl Transferase Deficiency. *Biochemical and Molecular Medicine*, *59*(1), 7–12. https://doi.org/10.1006/bmme.1996.0057

Lewis, E. M., Barnett, F. J., Freshwater, L., Hoberman, A. M., & Christian, M. S. (2002). Sexual Maturation Data for Crl Sprague-Dawley Rats: Criteria and Confounding Factors. *Drug and Chemical Toxicology*, *25*(4), 437–458. https://doi.org/10.1081/DCT-120014794

Panis, B., Gerver, W.-J. M., & Rubio-Gozalbo, M. E. (2007). Growth in treated classical galactosemia patients. *European Journal of Pediatrics*, *166*(5), 443–446. https://doi.org/10.1007/s00431-006-0255-4

Pyhtila, B. M., Shaw, K. A., Neumann, S. E., & Fridovich-Keil, J. L. (2015). Newborn Screening for Galactosemia in the United States: Looking Back, Looking Around, and Looking Ahead. In J. Zschocke, K. M. Gibson, G. Brown, E. Morava, & V. Peters (Eds.), *JIMD Reports, Volume 15* (pp. 79–93). Springer. https://doi.org/10.1007/8904_2014_302

Rasmussen, S. A., Daenzer, J. M. I., MacWilliams, J. A., Head, S. T., Williams, M. B., Geurts, A. M., Schroeder, J. P., Weinshenker, D., & Fridovich-Keil, J. L. (2020). A galactose-1-phosphate uridylyltransferase-null rat model of classic galactosemia mimics relevant patient outcomes and reveals tissue-specific and longitudinal differences in galactose

metabolism. *Journal of Inherited Metabolic Disease*, *43*(3), 518–528. https://doi.org/10.1002/jimd.12205

Schweitzer, S., Shin, Y., Jakobs, C., & Brodehl, J. (1993). Long-term outcome in 134 patients with galactosaemia. *European Journal of Pediatrics*, *152*(1), 36–43. https://doi.org/10.1007/BF02072514

Tang, M., Siddiqi, A., Witt, B., Yuzyuk, T., Johnson, B., Fraser, N., Chen, W., Rascon, R., Yin, X., Goli, H., Bodamer, O. A., & Lai, K. (2014). Subfertility and growth restriction in a new galactose-1 phosphate uridylyltransferase (GALT)—Deficient mouse model. *European Journal of Human Genetics*, *22*(10), 1172–1179. https://doi.org/10.1038/ejhg.2014.12

Vandamme, T. F. (2014). Use of rodents as models of human diseases. *Journal of Pharmacy & Bioallied Sciences*, *6*(1), 2–9. https://doi.org/10.4103/0975-7406.124301

Waggoner, D. D., Buist, N. R. M., & Donnell, G. N. (1990). Long-term prognosis in galactosaemia: Results of a survey of 350 cases. *Journal of Inherited Metabolic Disease*, *13*(6), 802–818. https://doi.org/10.1007/BF01800204

Walter, JH and Fridovich-Keil, JL (2008) Galactosemia. In: Valle D, Beaudet A, Vogelstein B (eds). The Online Metabolic & Molecular Bases of Inherited Disease. McGraw Hill; http://www.ommbid.com/.

Welling, L., Bernstein, L. E., Berry, G. T., Burlina, A. B., Eyskens, F., Gautschi, M., Grünewald, S., Gubbels, C. S., Knerr, I., Labrune, P., Lee, J. H. van der, MacDonald, A., Murphy, E., Portnoi, P. A., Õunap, K., Potter, N. L., Rubio-Gozalbo, M. E., Spencer, J. B., Timmers, I., … Bosch, A. M. (2017). International clinical guideline for the management of

classical galactosemia: Diagnosis, treatment, and follow-up. *Journal of Inherited Metabolic Disease*, *40*(2), 171–176. https://doi.org/10.1007/s10545-016-9990-5